

# Directing Close-Packing of Midnanosized Gold Nanoparticles at a Water/Hexane Interface

Yong-Kyun Park and Sungho Park\*

Department of Chemistry, BK21 School of Chemical Materials Science, and SKKU Advanced Institute of Nanotechnology, Sungkyunkwan University, Suwon 440-746, South Korea

Received December 8, 2007. Revised Manuscript Received January 11, 2008

This paper reports a method for assembling midnanosized Au nanoparticles ( $25 < d < 100$  nm) into close-packed 2D arrays with a high degree of local order. An in situ coating of Au nanoparticles with an alkanethiol surfactant can induce close-packed particle arrays when the nanoparticles are trapped at the interface. The film morphology was determined to be either monoparticulate or multiparticulate depending on the 1-dodecanethiol concentration. This paper reports on the optimum conditions for the formation of a close-packed 2D array by suggesting a phase diagram obtained from a plot of the 1-dodecanethiol concentration versus the nanoparticle diameter. When the diameter of Au nanoparticles was larger than ca. 40 nm, the full coverage of 1-dodecanethiols on the surface of nanoparticles was not enough to form close-packed nanoparticle arrays. The larger nanoparticles required the more 1-dodecanethiols to form a close-packed 2D array. This method also allows the nanoparticle surface to be coated asymmetrically with 1-dodecanethiols, which was confirmed qualitatively from contact angle measurements.

## 1. Introduction

The assembly of nanoparticles (NPs) into two- or three-dimensional structures has attracted considerable attention on account of their unique electronic and optical properties, which are determined by the particle size, interparticle spacing, and periodicity.<sup>1–7</sup> One of the best known approaches for constructing such structures is related to a self-assembly concept whereby a droplet of surfactant stabilized NPs evaporates in a controlled manner.<sup>8–12</sup> For two-dimensional (2D) arrays of metal NPs, hydrophobic surfactants with strongly adsorbing functional groups, such as alkanethiols, are often used to drive such assembly at the air/water interface. However, the formation of a 2D array using this approach has been limited to small metal NPs ( $d < 10$  nm).<sup>13</sup> It was suggested that an increase in van der Waals attraction and the loss of surfactant chain mobility

on the planar facets of NPs as a function of size are the reasons for such limits.<sup>13,14</sup> To overcome the size threshold, Wei et al. designed a new class of surfactants based on the framework of resorcinarene.<sup>13</sup> The bulk headgroup and several hydrocarbon tails per molecule spaced several angstroms apart allowed the assembly of large metal NPs ( $16 < d < 170$  nm) into 2D arrays. The high degree of configurational freedom per chain in the surfactant layer, which is related to steric repulsion between NPs, was the possible reason for ordering large NPs into 2D arrays.<sup>13,14</sup>

Recently, it was reported that hydrophilic NPs can be assembled into 2D arrays at water/oil interfaces by destabilizing the NPs by adding a low-dielectric solvent to an aqueous colloidal suspension.<sup>15–17</sup> When a particle is hydrophilic, it has a contact angle  $< 90^\circ$  at the water/oil interface and is suspended in the water phase. When its contact angle approaches  $90^\circ$ , the particle prefers to adsorb to the water/oil interface in order to decrease the interfacial energy between the water and oil. Previous reports have shown that the addition of alcohols causes the contact angle of NPs to approach  $90^\circ$ , and suggested that this plays an important role in NP entrapment at the interface.<sup>15,18</sup> Although it is possible to assemble NPs into 2D monolayers using this approach, the NPs are not close-packed, and inhomogeneous microscopic features are often observed. It has been reported that the disordering in the resulting NP

\* Corresponding author. E-mail: spark72@skku.edu.

- (1) Collier, C. P.; Saykally, R. J.; Shiang, J. J.; Henrichs, S. E.; Heath, J. R. *Science* **1997**, *277*, 1978–1981.
- (2) Andres, R. P.; Bein, T.; Dorogi, M.; Feng, S.; Henderson, J. I.; Kubiak, C. P.; Mahoney, W.; Osifchin, R. G.; Reifengerger, R. *Science* **1996**, *272*, 1323–1325.
- (3) Kim, S.-H.; Medeiros-Ribeiro, G.; Ohlberg, D. A. A.; Williams, R. S.; Heath, J. R. *J. Phys. Chem. B* **1999**, *103*, 10341–10347.
- (4) Yun, S.-H.; Yoo, S. I.; Jung, J. C.; Zin, W.-C.; Sohn, B.-H. *Chem. Mater.* **2006**, *18*, 5646–5648.
- (5) Liang, Z.; Susha, A.; Caruso, F. *Chem. Mater.* **2003**, *15*, 3176–3183.
- (6) Pileni, M. P. *J. Phys. Chem. B* **2001**, *105*, 3358–3371.
- (7) Giersig, M.; Mulvaney, P. *Langmuir* **1993**, *9*, 3408–3413.
- (8) Bigioni, T. P.; Lin, X.-M.; Nguyen, T. T.; Corwin, E. I.; Witten, T. A.; Jaeger, H. M. *Nat. Mater.* **2006**, *5*, 265–270.
- (9) Lin, X. M.; Jaeger, H. M.; Sorensen, C. M.; Klabunde, K. J. *J. Phys. Chem. B* **2001**, *105*, 3353–3357.
- (10) Narayanan, S.; Wang, J.; Lin, X.-M. *Phys. Rev. Lett.* **2004**, *93*, 135503.
- (11) Wang, Z. L. *Adv. Mater.* **1998**, *10*, 13–30.
- (12) Ohara, P. C.; Leff, D. V.; Heath, J. R.; Gelbart, W. M. *Phys. Rev. Lett.* **1995**, *75*, 3466–3469.
- (13) Kim, B.; Tripp, S. L.; Wei, A. J. *Am. Chem. Soc.* **2001**, *123*, 7955–7956.

- (14) Wei, A. *Chem. Commun.* **2006**, *15*, 1581–1591.
- (15) Reincke, F.; Hickey, S. G.; Kegel, W. K.; Vanmaekelbergh, D. *Angew. Chem., Int. Ed.* **2004**, *43*, 458–462.
- (16) Duan, H.; Wang, D.; Kurth, D. G.; Mohwald, H. *Angew. Chem., Int. Ed.* **2004**, *43*, 5639–5642.
- (17) Li, Y.-J.; Huang, W.-J.; Sun, S.-G. *Angew. Chem., Int. Ed.* **2006**, *45*, 2537–2539.
- (18) Reincke, F.; Kegel, W. K.; Zhang, H.; Nolte, M.; Wang, D.; Vanmaekelbergh, D.; Mohwald, H. *Phys. Chem. Chem. Phys.* **2006**, *8*, 3828–3835.

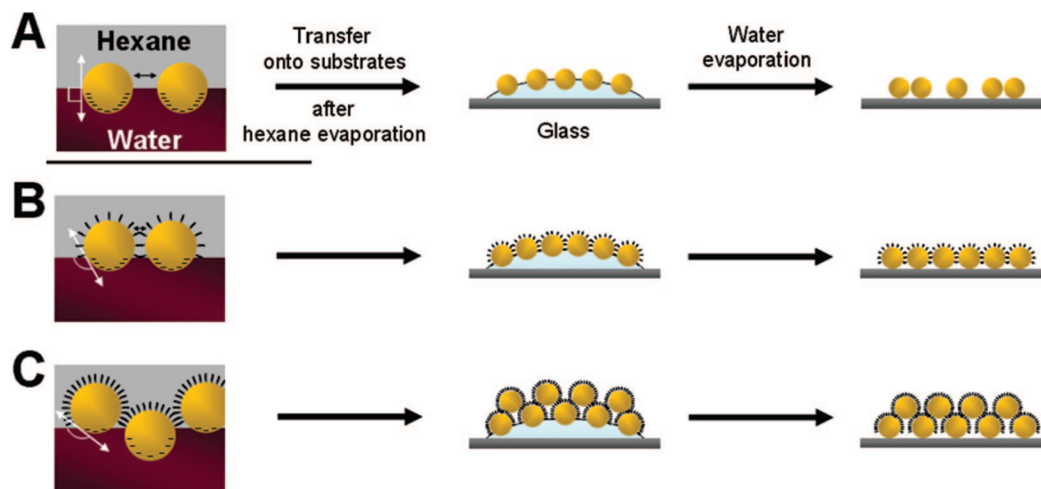


**Figure 1.** Schematic representation of the NP film formation. (A) NP film formation at a water/hexane interface and its transfer onto glass substrates after hexane evaporation. (B) As in scheme (A) except the presence of optimum amount of 1-dodecanethiols in a hexane phase for monolayer film. (C) As in scheme (A) except the presence of extra amount of 1-dodecanethiols in a hexane phase.

films are caused by the broad size distribution and competitive electrostatic repulsion against long-range van der Waals interactions.<sup>15–17</sup> This drawback can be overcome by reducing the electrostatic repulsion through an in situ coating of the NP surfaces with alkanethiols when the NPs were entrapped at the interface.<sup>19</sup> The aim of this study was to expand this strategy to midnanosized NPs ( $25 < d < 100$  nm) and show that large metal NPs can be assembled into close-packed 2D arrays at a water/hexane interface with alkanethiols. It was found that the concentration of alkanethiols in the hexane phase is important for controlling the formation of a NP array as a function of the NP size. The optimum concentration of alkanethiols for 2D arrays increased with increasing NP size. When the NP size was larger than a certain size ( $d > \text{ca. } 40$  nm), a full monolayer coverage of alkanethiol on the NP surface was not enough to induce a close-packed 2D arrays of NPs. This paper describes the optimum conditions that direct large gold NPs to self-assemble at a water/hexane interface into a close-packed 2D array.

## 2. Experimental Section

All chemicals were obtained from Aldrich and used as received. The Au colloid sol ( $d \approx 13 \pm 1.5$  nm) was prepared using a conventional methodology.<sup>20</sup> Briefly, 100 mL of a 1.0 mM aqueous  $\text{HAuCl}_4 \cdot 3\text{H}_2\text{O}$  solution was added to 100 mL of triply deionized water (Millipore), which was then boiled. Ten milliliters of a 38.8 mM aqueous solution of sodium citrate was added, which was then boiled for 20 min. A seed-mediated growth approach was used for large Au colloid sol. A volume of 4 mL of a 20 mM aqueous  $\text{HAuCl}_4 \cdot 3\text{H}_2\text{O}$  solution and 0.4 mL volume of a 10 mM  $\text{AgNO}_3$  solution were added to 170 mL of triply deionized water. Fifteen milliliters of the aforementioned 13 nm Au NP sol was added to the solution. Thirty milliliters of 5.3 mM ascorbic acid was then added slowly (0.6 mL/min) with constant stirring. The resulting NP diameter was determined to be  $29 \pm 3$  nm. When the seed amount was changed to 3 mL under the same experimental conditions, the resulting NP size was  $49 \pm 3$  nm. For a  $76 \pm 4$  nm

colloid sol, 1 mL of the seed solution was added. For  $94 \pm 5$  nm, 0.5 mL of the seed solution was used.

Field emission scanning electron microscopy (FESEM) and transmission electron microscopy (TEM) images were obtained using JEOL 7000F and JEOL JEM-3011, respectively. The experimental extinction spectra were collected on a Scinco S-3100 UV–vis spectrophotometer.

Twenty milliliters of an aqueous gold NP colloid was transferred to a Teflon cell (inner dimension,  $8.0 \times 4.0 \times 1.7$  cm), and 10 mL of hexane was added to the top of the colloid solution surface to form an immiscible water/hexane interface. A certain amount of 1-dodecanethiol was then added dropwise to the hexane layer, and there was no observable change in the colloid solution. Fifteen milliliters of ethanol was then added dropwise to the surface of the water/hexane layers (0.6 mL/min, using a mechanical syringe pump, KDS101 from kd Scientific Inc.), which led to NP trapping at the interface.

Depending on the amount of ethanol added, it was possible to tune the resulting two-dimensional area of the NP array. After forming the desired area of the NP array at the interfaces, the hexane layer was evaporated spontaneously. During this process, the NPs naturally assemble into close-packed islands, which lead to the appearance of a mirrorlike metallic sheen as a result of optical coupling of the NPs. These films could be transferred to a solid substrate by horizontal lifting for in-depth analysis of the film profile by FESEM and TEM.

## 3. Results and Discussion

Figure 1 shows a schematic diagram of the mechanism for NP assembly at a water/hexane interface with and without alkanethiols in the hexane phase. The driving force for the entrapment of NPs upon the ethanol addition is the decrease in interfacial energy between water and hexane through the assembly of NPs at the interface. This interfacial entrapment is mainly determined by the contact angle ( $\theta$ ) of the NP. When a particle is hydrophilic, it has a contact angle  $< 90^\circ$  at the interface, and is suspended in the aqueous phase. When the dielectric constant of medium is decreased by the addition of a miscible solvent with a lower dielectric constant, the surface charge of the charged particles gradually decreases as a function of the amount of solvent added. When ethanol is added, the surface charge density of the nanoparticles

(19) Park, Y.-K.; Yoo, S.-H.; Park, S. *Langmuir* **2007**, *23*, 10505–10510.

(20) Park, S.; Yang, P.; Corredor, P.; Weaver, M. J. *J. Am. Chem. Soc.* **2002**, *124*, 2428–2429.

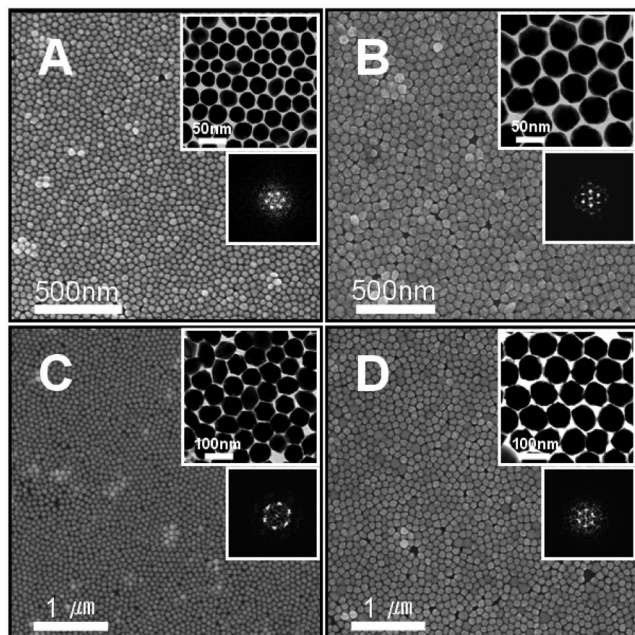


**Figure 2.** FESEM, TEM (upper right insets), and FFT (lower right insets) images of NP films transferred on silicon wafers (fore FESEM images) and copper TEM grid. The films were prepared in the presence of 1-dodecanethiol in a hexane layer, and using a variety of NPs with different size ( $d$ ), (A)  $29 \pm 3$ , (B)  $49 \pm 3$ , (C)  $76 \pm 4$ , and (D)  $94 \pm 5$  nm by following the represented scheme B in Figure 1.

decreased, which leads to the adsorption of NPs to the interface. The addition of ethanol to the aqueous phase decreases the surface charge of the NPs and increases the contact angle to almost  $90^\circ$ , which eventually leads to NP entrapment at the interface, as shown in Figure 1A. However, the residual surface charge density ( $\sigma$ ) keeps NPs apart to a certain distance. The addition of ethanol only to the water is not enough to decrease the  $\sigma$  value below a certain value. The residual double layer electrostatic repulsive force keeps the interfacial particle density low. When the water evaporates, the repulsive force disappears and the distance between the NPs decreases. The resulting NP film usually shows voids when the NP density on the surface is low, as previously reported in other studies.<sup>15–17</sup> The  $\sigma$  value needs to be further decreased in order to assemble NPs into close-packed arrays. The simple addition of a certain amount of alkanethiol in a hexane phase can play such a role in the assembly process. An in situ coating of the NP surface when the NPs are entrapped at the interface induces a further decrease in the  $\sigma$  value, which leads to an increase in the NP population density at the interface. The decrease of the  $\sigma$  value would be dependent on the degree of passivation of NPs with 1-dodecanethiol. Therefore, the concentration of 1-dodecanethiol in the hexane layer is quite important in terms of determining the density of entrapped NPs at the interface. The excess amount of 1-dodecanethiol in the hexane layer would suppress the desorption of thiol from the NP surface, which promotes the surface passivation and minimizes the surface charge. The subsequent evaporation of water after transferring onto the solid substrates results in close-packed NP films (Figure 1B). Figure 2 shows the FESEM and TEM images of the close-packed 2D arrays of the Au NPs as a function of the particle size, which was obtained by following

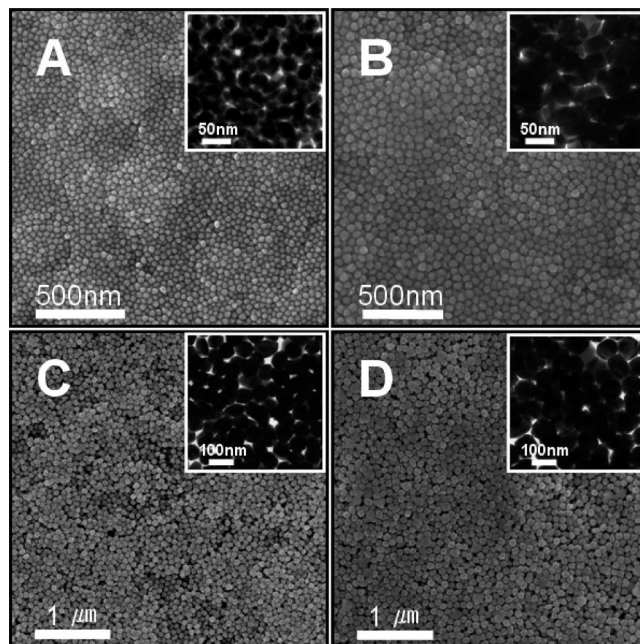


**Figure 3.** As in Figure 2, but for multilayer NP films with an extra amount of 1-dodecanethiols in a hexane phase. Films were prepared by following the represented scheme C in Figure 1.

the aforementioned experimental procedures with 1-dodecanethiols in a hexane phase. The FESEM and TEM images show the uniformity of the transferred arrays and the monoparticulate nature of the films, respectively, regardless of NP size ( $25 < d < 100$  nm). Each inset shows the corresponding fast Fourier transformation (FFT) images and reveals a close-packed array of Au NPs formed with high order locally. The order disappears when the FFT images included a large area, which is due to the inhomogeneous particle size distribution. Previously, Malvaney et al. reported that alkanethiol-stabilized Au NPs could be electrophoretically deposited onto carbon-coated copper grids.<sup>7</sup> From the TEM and FFT images, they found that an average core-to-core distance among the hexagonal close packed Au NPs is shorter than the calculated distance by considering the fully extended alkanethiol chain length. It indicates some interpenetration of the chains. A close analysis of our TEM images reveals the interparticle distance, ca. 2 nm for the investigated NP sizes, which was measured from the neighboring two boundaries. The interparticle distance does not vary significantly for the investigated Au NP sizes. The estimated length of 1-dodecanethiol when it is fully extended is ca. 1.8 nm.<sup>7</sup> Therefore, the shorter interparticle distance than the length of tip-to-tip assembly of two 1-dodecanethiol molecules indicates the presence of interdigitation of the chains.

A close-packed NP film was observed when the 1-dodecanethiol concentration in a hexane phase was increased to a certain level, as in the case with Figure 2, with the exception that the film thickness is approximately two monolayers. The FESEM images in Figure 3 show the high density of NPs on the substrates and the TEM images indicate the multilayer nature. A careful inspection of the TEM images revealed the double-layer characteristics of the films. When the amount of 1-dodecanethiol on the NP surface was

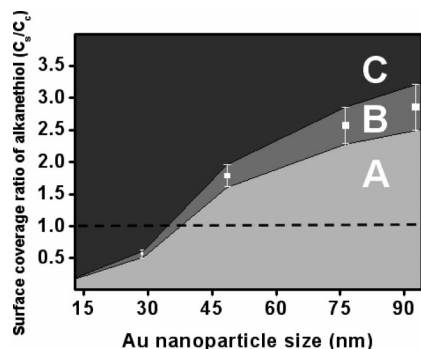


**Figure 4.** Phase diagram for NP film formation obtained from the plot, surface coverage ratio of 1-dodecanethiols versus particle diameter ( $C_s/C_c$ ,  $C_s$ , experimentally determined thiol concentration on NP surface;  $C_c$ , calculated thiol concentration for full coverage with a given size of NP, see text). The regions represent the experimental conditions for (A) the monoparticulate film with voids among NPs, (B) a close-packed NP film, and (C) multilayer NP film. Dashed traces represent the condition when  $C_s = C_c$ .

greater than the amount required for the 2D NP arrays, the attractive interaction between the NP and hexane would increase because of better surface passivation with 1-dodecanethiol, and the center of the NPs would move from the interface to the hexane phase. Then the interfacial energy will increase due to an increase in the open space at the interface, which can induce a second layer of NP entrapment at the interface in order to counterbalance the increase in interfacial energy. Figure 1C shows a schematic diagram of this mechanism. The complete NP phase transfer from water to hexane was not observed during the addition of ethanol. This is because the interaction energy between hexane and the 1-dodecanethiol coated NPs ( $25 < d < 100$  nm) is smaller than the interfacial stabilization energy ( $\Delta E_{\text{int}} \approx 1 \times 10^5 kT$  for  $d = 100$  nm,  $\Delta E_{\text{int}} \approx 1 \times 10^3 kT$  for  $d = 10$  nm).<sup>21</sup> Also, the attractive interaction among the entrapped NPs at the interface will counteract the NP phase transfer to hexane layer.

The optimal 1-dodecanethiol concentration on the NP surface depending on the NP size could be determined, and the corresponding phase diagram is shown in Figure 4. The concentration of adsorbed 1-dodecanethiols was examined by dividing the total number of 1-dodecanethiols by the total number of particles, by assuming the close-packing of NPs residing in a given area. For example, there will be  $1.04 \times 10^{11}$  particles (for NPs with  $d = 29$  nm) if the films form a close-packed monoparticulate structure in one square centimeter. If a volume of 10 mL of 1.0  $\mu\text{M}$  1-dodecanethiols (equivalent to ca.  $6.3 \times 10^{15}$  molecules) and NPs with  $d \approx 29 \pm 3$  nm are used, each NP would have ca.  $5.5 \times 10^3$  1-dodecanethiol molecules. The number of adsorbed molecules could be calculated assuming an even distribution of 1-dodecanethiols over the NP surface. In order to calculate the saturation coverage of 1-dodecanethiols as a function of the NP size, it was assumed that the 1-dodecanethiols form a close-packed monolayer with the van der Waals dimensions of the thiol headgroup ( $21.4 \text{ \AA}^2$ ) perpendicular to the

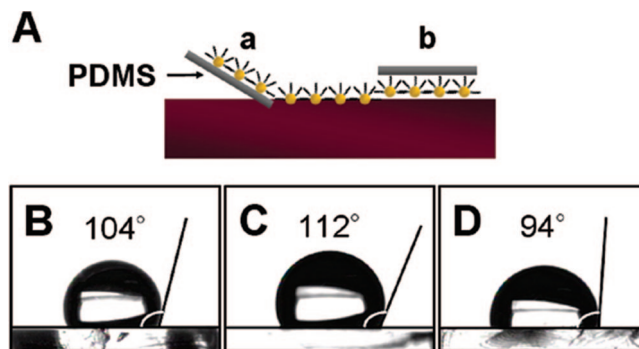


**Figure 5.** (A) NP film transfer on substrates from (a) bottom horizontal- and (b) top-lifting. (B–E) Contact angle measurements on (B) a bare PDMS slide and (C) a close-packed NP film prepared by horizontal lifting as described in (A)-a route, and on (D) a close-packed NP film prepared by top-lifting as described in (A)-b route.

surface.<sup>22</sup> This calculated full coverage of 1-dodecanethiols was set to  $C_c$  (each  $C_c$  value as a function of the particle size is 9687 (when  $d = 29$  nm), 27206 (when  $d = 49$  nm), 66880 (when  $d = 76$  nm), and 101775 (when  $d = 94$  nm)). The calculated surface coverage of 1-dodecanethiols from the added of 1-dodecanethiols amount was set to  $C_s$ . The surface coverage ratios,  $C_s/C_c$ , represent the relative amount of 1-dodecanethiols on the NP surface.  $C_s/C_c = 1$  indicates that the surface is fully covered by 1-dodecanethiols. If  $C_s/C_c < 1$ , the surface is partially covered with 1-dodecanethiols. If  $C_s/C_c > 1$ , the surface is overcoated. Region B in Figure 4 shows the optimal conditions for the close-packing of NPs as a function of size. Each region in A and C shows a monoparticulate film with void domains and a multiparticulate film, respectively. One noticeable feature is that when the particle size is large ( $d > \text{ca. } 40$  nm), full coverage of 1-dodecanethiol on the NP surface is not enough to decrease the surface charge ( $\sigma$ ) to a certain level for close-packed monoparticulate film formation. As shown in Figure 1B, the center of the NP needs to be shifted to the hexane phase for close-packing after drying. The interfacial stabilization energy  $\Delta E_{\text{int}}$  is proportional to the particle size ( $r^2$ ).<sup>21</sup> Therefore, as the particle size becomes larger it will become increasingly difficult to move the center of an immobilized NP to the hexane phase. This trend is quite evident in the Figure 4. Another concern with this consideration is related to the distribution of 1-dodecanethiols on the NP surface. 1-dodecanethiol is slightly soluble in water. Hence, it is likely that most of the 1-dodecanethiols adsorbed on the NPs will reside in the hexane phase. At the current stage, there is no direct analytical method that can confirm this statement. However, the asymmetrical coating of NPs with 1-dodecanethiols can be confirmed qualitatively. The films can be transferred to a hydrophobic polydimethylsiloxane (PDMS) substrate by horizontal lifting (immersing the substrate below the NP film and then lifting it horizontally) after hexane evaporation. This would result in the NP surface in a hexane phase being exposed to air. In contrast, these NP films can be transferred to a PDMS substrate by bringing the substrate parallel to the water surface and touching the floating NP films (i.e., Langmuir–Schaefer technique). The resulting NP films are expected to have a surface exposed to the air that was previously in the water phase. The instant contact angle

(21) Binder, W. H. *Angew. Chem., Int. Ed.* **2005**, *44*, 5172–5175.

(22) Sellers, H.; Ulman, A.; Shnidman, Y.; Eilers, J. E. *J. Am. Chem. Soc.* **1993**, *115*, 9389–9401.

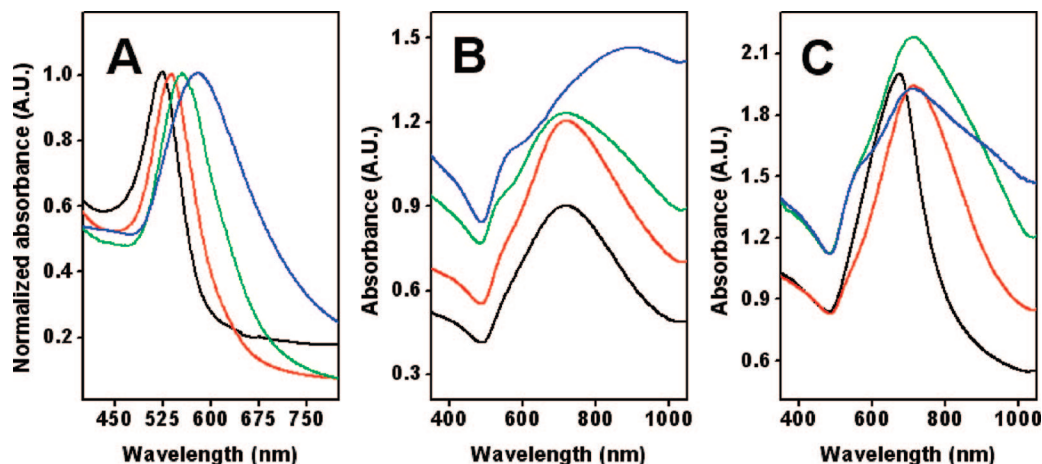


**Figure 6.** UV-vis absorption spectra for different sized gold NPs (A) in a water phase, (B) on a glass slide with monoparticulate close-packed film, and (C) on a glass slide with multiparticulate film. Particle size: (black line)  $29 \pm 3$ , (red line)  $49 \pm 3$ , (green line)  $76 \pm 4$ , and (blue line)  $94 \pm 5$  nm.

of a  $3 \mu\text{L}$  water droplet was then measured. The measured contact angle of the bare PDMS substrate was approximately  $\sim 104^\circ$ . The measured contact angle on the former NP film (prepared with NP's  $d \approx 13 \pm 1.5$  nm) was  $112^\circ$ , and the latter was  $94^\circ$ , which confirms the asymmetric coating of 1-dodecanethiols on the NP surface. It is noteworthy that the measured contact angle difference does not originate from the roughness difference because the samples were prepared with the identical experimental conditions. The surface of the NP films, which was facing toward the hexane phase, showed an increase in contact angle compared with the bare PDMS substrate. This was attributed to the presence of 1-dodecanethiol on the surface. In contrast, the contact angle on the surface in contact with the water phase decreased, showing an even lower level than the bare PDMS substrate. The absence of 1-dodecanethiol and the hydrophilic nature of these NPs induced a decrease in contact angle. It is qualitatively clear that the majority of 1-dodecanethiols resides on the NP surface in the hexane phase.

The surface plasmon characteristics of these films are also of considerable interest. Figure 6A shows the extinction spectra of a NP suspension in water as a function of size. All the spectra were obtained in transmission mode, without polarization of the light. We estimated the fill factor for each NP film, and found that 79.8% fill factor (area fraction) for NP with  $d \approx 29$  nm, 80.5% for  $d \approx 49$  nm, 80.0% for  $d \approx 76$  nm, 78.0% for  $d \approx 94$  nm. The substrate was a cover glass slide with refractive index, 1.514 (from Marienfeld, microscopy cover glass). As already known both experimentally and theoretically, a consistent red-shift in the peak position was observed with increasing particle size.<sup>23,24</sup> The peak positions were ca. 523, 537, 555, and 579 nm for Au NPs,  $29 \pm 3$ ,  $49 \pm 3$ ,  $76 \pm 4$ , and  $94 \pm 5$  nm in diameter, respectively (Figure 6A). The resulting 2D arrays of each NP film showed the corresponding UV-vis spectra, as shown in Figure 6B. The extinction density increased with increasing particle size due to large absorption and scattering cross-section. The broad tail in the near-infrared region was

attributed to optical coupling between NPs. The larger NPs showed stronger coupling in the near-infrared region, which is evident from the broader band shape in the long wavelength spectral window. The size-dependent broadening of the extinction band is noteworthy because it represents the insulator-to-metal transition in the NP films or the retardation of the induced dipole within the film.<sup>1,13</sup> As the coupling increase among Au NPs, the effective size of the Au NPs is larger than the wavelength of light. It will lead to the variation of induced dipole moment across the film. Then, it is expected that the dephasing of the induced dipole within the Au NP films would occur, which is represented by band broadening. The ratio ( $\delta/d$ ) between the interparticle-distance ( $\delta$ ) and the NP diameter ( $d$ ) decreases with increasing NP size, as determined from the TEM images in Figure 2. This observation is related to size-dependent extinction band broadening. In contrast, the corresponding multilayer NP films that were prepared under the experimental conditions shown in the region C in Figure 4 have different extinction band shapes, as shown in Figure 6C. The peak position shifted to a shorter wavelength and the bandwidth at half-maximum became narrower compared with the corresponding monoparticulate films. This is due to the high concentration of 1-dodecanethiols between NPs, which decreases the degree of NP surface plasmon coupling. The decrease in optical coupling contributes to a peak-shift to a shorter wavelength as the molecular shell thickness increases. A similar trend was observed in the silica-coated gold NP system.<sup>25</sup> The absorption spectra of a series of films showed a consistent blue-shift as the silica shell thickness was increased in a given NP size.<sup>25</sup> These results are consistent with the data obtained in this study. The peak shapes of the multiparticulate films resemble those in the aqueous phase with the exception that the peaks are at a longer wavelength. The change in dielectric medium is the reason for such a red-shift in the peak positions compared with colloids in the aqueous phase.

Suitable surfactants are not restricted to 1-dodecanethiols. The same experiment was carried out with different mol-

(23) Kreibig, U.; Vollmer, M. *Optical Properties of Metal Clusters*; Springer: New York, 1995.

(24) Mulvaney, P. *Langmuir* **1996**, *12*, 788–800.

(25) Ung, T.; Liz-Marzan, L. M.; Mulvaney, P. *J. Phys. Chem. B* **2001**, *105*, 3441–3452.

ecules such as 1-octanethiols and 1-hexadecanethiols, which have strongly adsorbing thiol functional groups. The optimum amount of surfactant for the 2D arrays tended to decrease with increasing chain length of the surfactant due to an increase in the degree of hydrophobic interactions, as expected. It was not possible to form a close-packed NP arrays when weakly adsorbing surfactants, such as normal alkanecarboxylic acids were used instead. The resulting NP films showed voids between NPs even though it showed a monoparticulate nature with local close-packing (data not shown). The weak adsorption of the surfactant might not be able to induce a further decrease in surface charge ( $\sigma$ ) sufficient for 2D arrays.

#### 4. Conclusion

This paper reports a method for assembling midnanosized Au NPs ( $25 < d < 100$  nm) into a close-packed 2D arrays with high local orderliness. An in situ coating of NPs with an alkanethiol surfactant when the NPs were entrapped at the interface could induce close-packed particle arrays. The key feature is the decrease in the surface charge of NPs

through the adsorption of alkanethiols. The film morphology was determined to be monoparticulate or multiparticulate depending on the concentration of alkanethiols. The assembly of NPs in the midnanometer size window is important in terms of utilizing their size-dependent characteristics, such as high surface plasmon coupling for surface enhanced Raman spectroscopy, or higher order surface plasmon coupling (for example, Ag NPs), which have not been observed with smaller metal NPs.<sup>26</sup> In particular, this method will have great potential for related applications in the functionalization and modification of NP surfaces at a specific face.

**Acknowledgment.** This work was supported by a Korea Research Foundation Grant funded by the Korean Government (MOEHRD, KRF-2005-005-J11902, and KRF-C00050) and the Korea Science and Engineering Foundation (R01-2006-000-10426-0-2006).

CM703498Y

---

(26) Malynych, S. Chumanov, G. *J. Am. Chem. Soc.* **2003**, *125*, 2896–2898.